Fabrication of Photoluminescent Dyes/Poly(acrylonitrile) Coaxial Nanotubes Using Vapor Deposition Polymerization

Kyung Jin Lee, Joon Hak Oh, Younggeun Kim, and Jyongsik Jang*

Hyperstructures Organic Materials Research Center and School of Chemical and Biological Engineering, College of Engineering, Seoul National University, Shinlimdong 56-1, Seoul, 151-742 Korea

Received May 16, 2006. Revised Manuscript Received August 17, 2006

Poly(acrylonitrile) (PAN) nanotubes with tunable wall thickness were successfully fabricated using a modified vapor deposition polymerization technique. To enhance the uniformity, heptane was employed as a nonreactive solvent. It is revealed that the heptane vapor in the reaction vessel plays an important role for producing nanotubes with tunable and uniform wall thickness. In addition, photoluminescence dyes such as pyrene for blue emission and rhodamine B for red emission were employed as host materials. These dyes were loaded into the inner surface of the PAN nanotubes and effectively encapsulated with a supplemental PAN layer. Confocal laser scanning microscopy images confirmed the successful fabrication of PAN−dye−PAN nanotubes without phase separation of the organic dyes. The photoluminescent analysis demonstrated the effective confinement of pyrene as well as rhodamine B in the PAN layer with a varying concentration of pyrene and rhodamine B as a multi-emission polymer nanotube.

Introduction

One-dimensional (1-D) nanostructures have attained great interest due to their potential applications for optics, electronics, and so forth.[1−4] During the past decade, various materials such as polymers, metals, semiconductors, and carbon have been used to produce 1-D structures via template-based methods, layer-by-layer methods, and self-assembly methods.[5−12] The 1-D nanocomposites have also attracted considerable attention because the nanocomposites display unique properties which are different from those of bulk composites. To date, a diverse combination of materials has been adapted for producing 1-D nanocomposites: carbon nanotubes and fullerene derivatives containing metal or semiconductor nanoclusters, semiconductors with multiple layers, and inorganic nanotubes impregnated with nanoparticles.[13−27]

Among those, 1-D nanocomposites having useful optical properties is one of the most important subjects because of their promising applications in highlighted areas including optical devices and protein and DNA sensing.[28−31] Recently, Bai et al. demonstrated the fabrication of TiO_2-based composite nanotubes with CdS and Au nanoparticles using layer-by-layer techniques,[32] and Wu et al. reported the preparation of silica nanotubes containing fluorescent CdSe/ZnS and their biological application.[33] On the other hand, organic dyes have been less selected to fabricate composite nanotubes owing to their poor thermal and chemical stability, despite their high quantum efficiency.[34−36]

* Corresponding author. E-mail: jsjang@plaza.snu.ac.kr. Fax: 82 2 888 7295. Tel.: 82 2 880 7069.

(1) Bauner, L. A.; Birenbaum, N. S.; Meyer, G. J. *J. Mater. Chem.* **2004**, *14*, 517.
(2) Feng, L.; Li, S.; Li, Y.; Li, H.; Zhang, L.; Zhai, J.; Song, Y.; Liu, B.; Jiang, L.; Zhu, D. *Adv. Mater.* **2002**, *14*, 1857.
(3) Kong, J.; Franklin, N. R.; Zhou, C.; Chapline, M. G.; Peng, S.; Cho, K.; Dai, H. *Science* **2000**, *287*, 622.
(4) Jang, J. *Adv. Polym. Sci.* **2006**, *199*, 189.
(5) Lahav, M.; Sehayek, T.; Vaskevich, A.; Rubinstein, I. *Angew. Chem., Int. Ed.* **2003**, *42*, 5576.
(6) Lee, J.-K.; Koh, W.-K.; Chae, W.-S.; Kim, Y.-R. *Chem. Commun.* **2002**, 138.
(7) Bockrath, M.; Cobden, D. H.; McEuen, P. L.; Chopra, N. G.; Zettl, A.; Thess, A.; Smalley, R. E. *Science* **1997**, *275*, 1922.
(8) Morales, A. M.; Lieber, C. M. *Science* **1998**, *279*, 208
(9) Huczko, A. *Appl. Phys. A* **2000**, *70*, 365.
(10) Wang, X.-S.; Winnik, M. A.; Manners, I. *Angew. Chem., Int. Ed.* **2004**, *43*, 3703.
(11) Jang, J.; Lee, K. J.; Kim, Y. *Chem. Commun.* **2005**, 3847.
(12) Jang, J.; Yoon, H. *Adv. Mater.* **2004**, *16*, 799.
(13) Gao, M.; Huang, S.; Dai, L.; Wallace, G.; Gao, R.; Wang, Z. *Angew. Chem., Int. Ed.* **2000**, *39*, 3664.
(14) Endo, M.; Muramatsu, H.; Hayashi, T.; Kim, Y. A.; Terrones, M.; Dresselhaus, M. S. *Nature* **2005**, *433*, 476.
(15) Ma, R.; Bando, Y.; Sato, T. *Chem. Phys. Lett.* **2001**, *14*, 1.
(16) Sreekumar, T. V.; Liu, T.; Min, B. G.; Guo, H.; Kumar, S.; Hauge, R. H.; Smalley, R. E. *Adv. Mater.* **2004**, *16*, 58.
(17) Luo, L.-B.; Yu, S.-H.; Qian, H.-S.; Zhou, T. *J. Am. Chem. Soc.* **2005**, *127*, 2822.
(18) Li, L.-J.; Nicholas, R. J.; Chen, C.-Y.; Darton, R. C.; Baker, S. C. *Nanotechnology* **2005**, *16*, S202.
(19) Zhi, C. Y.; Zhong, D. Y.; Wang, E. G. *Chem. Phys. Lett.* **2003**, *381*, 715.
(20) Bao, J.; Tie, C.; Xu, Z.; Suo, Z.; Zhou, Q.; Hong, J. *Adv. Mater.* **2002**, *14*, 1483.
(21) Li, Y.; Bando, Y.; Golberg, D. *Adv. Mater.* **2004**, *16*, 93.
(22) Wu, J. J.; Liu, S. C.; Wu, C.-T.; Chen, K.-H.; Chen, L.-C. *Appl. Phys. Lett.* **2002**, *81*, 1312.
(23) Guo, Y.-G.; Wan, L.-J.; Bai, C.-L. *J. Phys. Chem. B* **2003**, *107*, 5441.
(24) Sun, C.-L.; Chen, L.-C.; Su, M.-C.; Hong, L.-S.; Chyan, O.; Hsu, C.-Y.; Chen, K.-H.; Chang, T.-F.; Chang, L. *Chem. Mater.* **2005**, *17*, 3749.
(25) Deepak, F. L.; Vanita, P. V.; Govindaraj, A.; Rao, C. N. R. *Chem. Phys. Lett.* **2003**, *374*, 314.
(26) Jiang, L.; Gao, L. *Chem. Mater.* **2003**, *15*, 2848.
(27) Yang, B.; Kamiya, S.; Shimizu, Y.; Koshizaki, N.; Shimizu, T. *Chem. Mater.* **2004**, *16*, 2826−2831
(28) Qian, H.-S.; Yu, S.-H.; Luo, L.-B.; Gong, J.-Y.; Fei, L.-F.; Liu, X.-M. *Chem. Mater.* **2006**, *18*, 2102.
(29) Qi, Y.; Chen, P.; Wang, T.; Hu, X.; Zhou, S. *Macromol. Rapid Commun.* **2006**, *27*, 356.
(30) Sanchez, C.; Lebeau, B.; Chaput, F.; Boilot, J.-P. *Adv. Mater.* **2003**, *15*, 1969.
(31) Kim, G.-M.; Wutzler, A.; Radusch, H.-J.; Michler, G. H.; Simon, P.; Sperling, R. A.; Parak, W. J. *Chem. Mater.* **2005**, *17*, 4949.
(32) Guo, Y.-G.; Hu, J.-S.; Liang, H.-P.; Wan, L.-J.; Bai, C.-L. *Adv. Funct. Mater.* **2005**, *15*, 196.
(33) Chen, C.-C.; Liu, Y.-C.; Wu, C.-H.; Yeh, C.-C.; Su, M.-T.; Wu, Y.-C. *Adv. Mater.* **2005**, *17*, 404.

10.1021/cm0611542 CCC: $33.50
Published on Web 09/26/2006

The porous membrane mediated method has several advantages to obtaining 1-D nanocomposites. The excellent orientation and confinement of the products make it possible to introduce host materials into tailored positions.[37−39] However, it is still a challenging task to develop a facile and novel method to prepare such 1-D nanocomposite materials. Generally, polymer nanotubes have been prepared using melt and solution based methods.[40] In these approaches, the possible capillary condensation and the strong interfacial tension between monomer and template make it difficult to realize nanotubes with thin-wall thickness and open pores. Recently, to overcome these drawbacks, we have developed fabrication methods for producing conducting polymer nanotubes using an anodic aluminum oxide (AAO) membrane with vapor deposition polymerization (VDP).[41−45] This technique constitutes a facile method to produce open pore polymer nanotubes with tunable wall thickness and provides an effective platform to introduce foreign materials into polymer nanotubes, resulting in polymer coaxial nanotubes with diverse functionality.

On the other hand, it is still difficult to fabricate vinyl polymer nanotubes via the VDP method, because the polymerization mechanism of vinyl monomers is more intricate than that of conducting polymers.[41] In general, vinyl monomers are initiated and propagated by a radical initiator, and the morphological control of vinyl polymer nanomaterials is difficult compared to the conducting polymer nanomaterials.[46−48] Herein we report a novel fabrication method for PAN (poly(acrylonitrile)) nanotubes with tunable wall thickness using VDP. Heptane is used as a nonreactive vapor to enhance the wall uniformity of the PAN nanotubes. The well-defined and uniform polymer nanotube provides the functional platform for the introduction of host materials. Dye-containing coaxial nanotubes were also successfully fabricated through dipping the AAO containing PAN nanotube in organic dye solution. The confocal laser scanning microscopy (CLSM) images, the transmission electron microscopy (TEM) images, and the photoluminescence (PL) spectra of the photoluminescent dye/PAN coaxial nanotubes confirmed the effective confinement of the organic dyes.

(34) Johansson, A.; Windenkvist, E.; Lu, J.; Boman, M.; Jansson, U. *Nano Lett.* **2005**, *5*, 1603.
(35) Muller, M.; Zentel, R.; Maka, T.; Romanov, S. G.; Torres, C. M. S. *Chem. Mater.* **2000**, *12*, 2508.
(36) Yang, Q.; Xu, W.; Tomita, A.; Kyotani, T. *J. Am. Chem. Soc.* **2005**, *127*, 8956.
(37) Kowollik, C. B.; Dalton, H.; Davis, T. P.; Stenzel, M. H. *Angew. Chem., Int. Ed.* **2003**, *42*, 3664.
(38) Zhang, X.; Ju, W.; Gu, M.; Meng, X.; Shi, W.; Zhang, X.; Lee, S. *Chem. Commun.* **2005**, 4202.
(39) Martin, C. R.; *Chem. Mater.* **1996**, *8*, 1739.
(40) Cepak, V. M.; Martin, C. R. *Chem. Mater.* **1999**, *11*, 1363.
(41) Jang, J.; Oh, J. H. *Chem. Commun.* **2004**, 882.
(42) Jang, J.; Lim, B.; Choi, M. *Chem. Commun.* **2005**, 4214.
(43) Jang, J.; Lim, B. *Angew. Chem., Int. Ed.* **2003**, *42*, 5600.
(44) Jang, J.; Ko, S.; Kim, Y. *Adv. Funct. Mater.* **2006**, *16*, 754.
(45) Lellouche, J.; Govindaraji, S.; Joseph, A.; Jang, J.; Lee, K. J. *Chem. Commun.* **2005**, 4357.
(46) Steinhart, M.; Wehrspohn, R. B.; Gosele, U.; Wendorff, J. H. *Angew. Chem., Int. Ed.* **2004**, *43*, 1334.
(47) Masuda, H.; Fukada, K. *Science* **1995**, *268*, 1466.
(48) Parthasarathy, R. V.; Phani, K. L. N.; Martin, C. R. *Adv. Mater.* **1995**, *7*, 896.

Scheme 1. Schematic Diagram of Fabrication of PAN Nanotubes and PAN/Dye/PAN Coaxial Nanotubes[a]

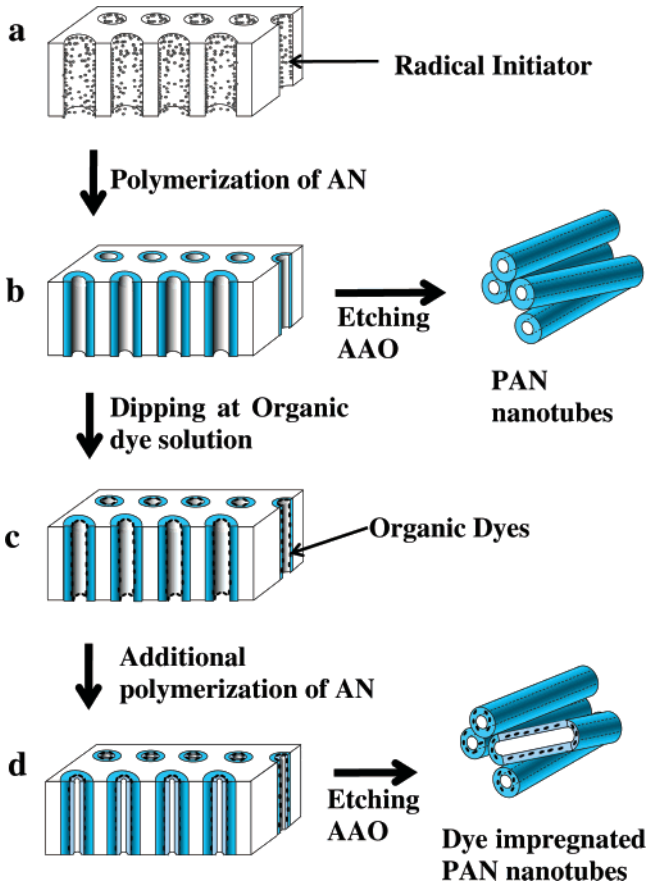

[a] (a) AAO membrane, (b) PAN impregnated AAO membrane, (c) dye dipped PAN nanotubes, and (d) multilayer coaxial nanotube of PAN/dye/PAN nanotubes.

Experimental Section

Materials. Porous anodic membranes with a pore diameter of 100 nm and a thickness of 60 μm were obtained from Wattman Co. All reactants including acrylonitrile (AN), pyrene, rhodamine B, heptane, hydrochloric acid, and methanol were purchased from Sigma Aldrich Co. The AN (monomer) was refined with an inhibitor removal column, and the other reactants were used without further purification. 2,2-Azo-bis-(2,4-dimethylvaleronitrile) purchased from Wako Co. was employed as a radical initiator.

Fabrication of PAN Nanotubes. The overall synthetic procedure is illustrated in Scheme 1. The AAO template was placed in a reaction vessel equipped with a sealing apparatus and a monomer-loading reservoir. The reaction chamber was evacuated at room temperature until inner pressure reached up to 10^{-2} Torr. The heptane solution containing a radical initiator was injected into the reaction vessel, and the AAO was wetted by the initiator/heptane solution (step a). In the typical synthetic procedure, 0.02 g of initiator was dissolved in 0.6 mL of heptane. AN monomer (0.1−0.6 mL) was fed into the reactor, and VDP was carried out at 70 °C for 6 h (step b). In addition, the wall thickness of the nanotubes could be tuned by adjusting the volume ratio of the monomer/heptane. The AAO template was removed with a 4 M hydrochloric aqueous solution. A suspension involving the PAN nanotubes was diluted, and the final products were obtained after the precipitation process.

Fabrication of PAN−Dye−PAN Nanotubes. After polymerization (without the etching process), the AAO membranes were soaked in a dye solution (step c). Pyrene and rhodamine B could

be dissolved in methanol/toluene (50:50, v/v) with the desired concentration. The dyes were loaded into the inner site of the PAN nanotubes. The upper and bottom layers of the AAO were polished with a fine sandpaper to prevent pores of the AAO from closing by residual dyes. Additional VDP of PAN was conducted to protect the organic dyes from the etching solution. Additional VDP includes the process of AAO wetting with the radical initiator and injecting the monomer. Then, the AAO membrane was dissolved in a HCl aqueous solution (4 M), and excess water was added to dilute the solution. Finally, the dye-embedded PAN nanotubes were precipitated (step d).

Characterization. TEM analysis was performed with a JEOL JEM-200CX. In the sample preparation, nanomaterials diluted in ethanol were cast onto the copper grid. Fourier transform infrared (FT-IR) spectra were recorded on Bomem MB 100 spectroscope in transmission mode at a resolution of 4 cm^{-1}. The FT-IR spectra were obtained via conventional KBr pellet methods with the final product precipitated and dried in a vacuum oven. The ultraviolet/visible (UV−vis) spectrum was taken with a Perkin-Elmer Lambda-20 spectrometer at a resolution of 1 nm. PL spectra were collected with a Shimadzu RF-5301 PC spectrofluorophotometer with a resolution of 1 nm. To obtain the UV−vis and PL spectra, precipitated and dried products (powder state) were dispersed in spectroscopic grade methanol. Fluorescence images were taken with a Carl Zeiss-LSM510 confocal laser scanning microscope.

Result and Discussion

TEM images of the PAN nanotubes prepared by VDP were presented in Figure 1. The PAN nanotubes with different wall thicknesses could be obtained by controlling the volume ratio of monomer/nonreactive vapor (heptane) fed into the reaction chamber. TEM images show that thickness and length of the nanotubes are in good agreement with the pore size (100 nm) of the AAO template and membrane thickness (60 μm). The PAN nanotubes retained a very thin wall thickness and open pores. The wall thicknesses of the PAN nanotubes were (a) 12 ± 2 nm, (b) 25 ± 2 nm, and (c) 38 ± 3 nm, when the volume ratios of the AN/monomer were (a) 0.15 mL/0.45 mL, (b) 0.30 mL/0.30 mL, and (c) 0.45 mL/0.15 mL, respectively. In addition, the inner and outer surface of nanotubes exhibited very smooth and uniform. In this system, the heptane played important roles in polymer nanotube formation with uniform wall thickness: (1) a dispersant of radical initiator and (2) a nonreactive vapor to enhance the wall uniformity of nanotube. Because the radical initiator is in the powder state, it is difficult to adsorb it into the AAO channel with homogeneity. Monodisperse adsorption of radical initiator was achieved by wetting the AAO with initiator/heptane solution, and the vaporized heptane can enhance the uniformity of the polymer nanotube wall. When the VDP was performed without the heptane vapor, PAN nanotubes with ill-defined morphologies were obtained. On the other hand, the PAN nanotubes with highly uniform wall thickness could be obtained using heptane vapor. During the polymerization process, the nonreactive heptane vapor can act as a heat reservoir in the reaction chamber.[49] Furthermore, heptane would be located at an inner location of AAO channels compared to AN monomers because of their hydrophobicity. Therefore, the PAN tubular structure could be readily obtained by this synthetic method.

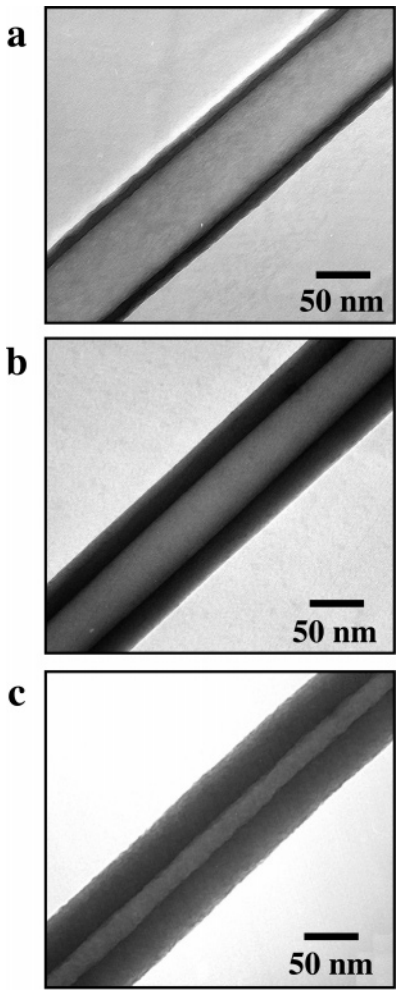

Figure 1. (a−c) TEM images of PAN nanotubes as a function of AN/heptane volume ratio: (a) 0.15 mL/0.45 mL, (b) 0.30 mL/0.30 mL, and (c) 0.45 mL/0.15 mL.

A FT-IR spectroscopic analysis was conducted to confirm the polymerization of AN monomer (Figure 2a). The FT-IR spectrum of the PAN nanotubes exhibited the characteristic PAN peaks of the C−H symmetric stretching vibration at at 2943 cm^{-1} and 2872 cm^{-1}. The band of 2245 cm^{-1} is attributed to the C≡N stretching vibration. Importantly, the C=C stretching peak at 1620 cm^{-1} in the AN monomer completely disappeared after polymerization. These results demonstrate the successful polymerization of AN.

The UV−vis investigation is also performed to characterize the monomer and polymer. As shown in the UV−vis spectrum of AN monomer in heptane (Figure 2b), the absorption peak is related with the n−π* transition at 225 nm (red dashed line). When the monomer is dissolved in a polar solvent such as methanol, *hypsochromic* shift occurs (about 3 nm), which can be the evidence that the n−π* transition is responsible for this absorption peak. The peak shift is attributed to lowering the energy level of the nonbonding orbital with increasing solvent polarity and hydrogen bonding between monomer molecule and solvent.[50] When the polymer (PAN) is dispersed in heptane, the broad absorption peak appears at 278 nm. In the case of methanol (polar solvent), *hypsochromic* shift (∼10 nm) is also observed

(49) Odian, G. *Principles of polymerization*, 3rd ed.; John Wiley & Sons: New York, 1991; p 286.

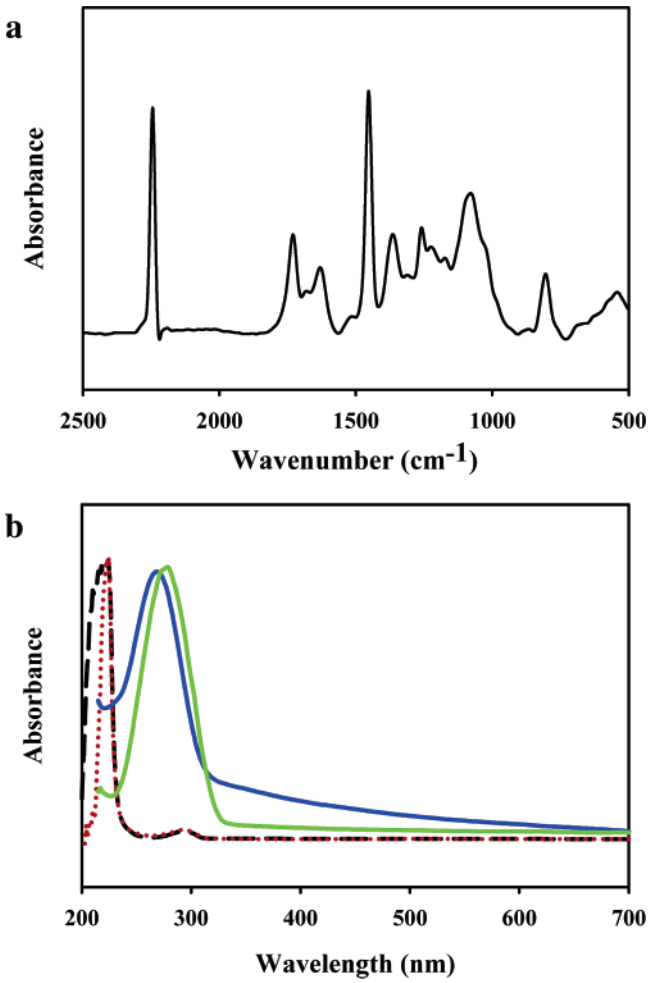

Figure 2. (a) FT-IR spectrum of PAN nanotubes and (b) UV−vis absorption spectra of AN monomer in methanol (black dashed line) and heptane (red dotted line) and PAN nanotubes in methanol (blue solid line) and heptane (green solid line).

at the UV−vis absorption of the PAN nanotube. In addition, these PAN nanotubes have no arresting absorption peaks in visible range (300−700 nm). Though bulk PAN is translucent in visible ranges, PAN nanomaterials are transparent in the wavelength range of 300−700 nm as shown in UV−vis spectra of PAN nanotubes. Therefore, the PAN nanotube does not restrain the emission flux of organic dye.

We have attempted to fabricate the PAN/dye nanotubes by simply dipping the AAO into the dye solution. Under these experimental conditions, the organic dyes were successfully encapsulated into the polymer layer. At first, the TEM image of PAN/rhodamine B/PAN coaxial nanotubes is displayed in Figure 3a. The wall of nanotubes is composed of two layers. The wall thickness of the first-synthesized PAN nanotubes is kept to be very thin, about 15 nm, to introduce host materials. The wall thickness of coaxial nanotubes is measured to be approximatly 30 nm, which is about a double of the wall thickness of the first layer. Tubular structure could be maintained after the dye-dipping process and additional VDP, through controlling the amount of loaded monomer. Figure 3b shows a three-dimensional (3D)

(50) Skoog, D. A.; Holler, F. J.; Nieman, T. A. *Principles of Instrumental Analysis*, 5th ed.; Saunders College Publishing: Philadelphia, 1998; p 332.

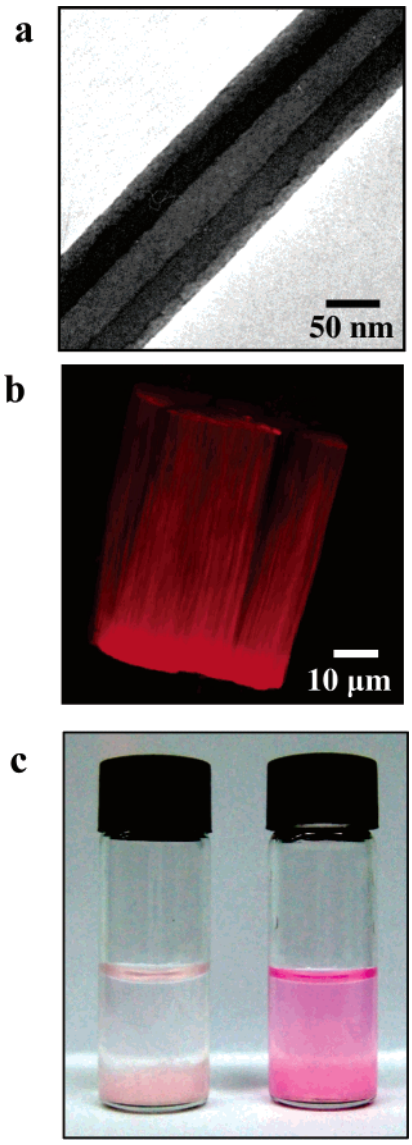

Figure 3. (a) TEM image of PAN/rhodamine B/PAN coaxial nanotubes, (b) 3D CLSM image of PAN/rhodamine B/PAN nanotubes, and (c) photograph of PAN/rhodamine B and PAN/rhodamine B/PAN coaxial nanotubes in water.

CLSM image of the PAN/rhodamine B/PAN coaxial nanotubes, excited by a 543 nm laser. The 3D CLSM images were obtained via collecting 24 Z sections. The CLSM image presents that the PAN/rhodamine B/PAN coaxial nanotube have the PL property of red emission and that it is restricted within the polymer nanotubes. Judging from these data, the PL dye is successfully embedded in the PAN layer without phase separation and deterioration. In this system, the photoluminescent dyes were entrapped by two PAN layers. If the reiterated-VDP process was deficient, the organic dyes have been dissolved into the etching solution during the AAO etching process. An additional layer at an inner location of the nanotubes is required to protect the organic dyes. Figure 3c shows photographs of PAN/rhodamine B nanocomposite (right) with one PAN layer and PAN/rhodamine B/PAN nanocomposite with double layered PAN (left), which is dispersed in an etching solution (HCl aqueous solution). The photograph in Figure 3c presents that the rhodamine B is effectively entrapped by the PAN layer, whereas rhodamine

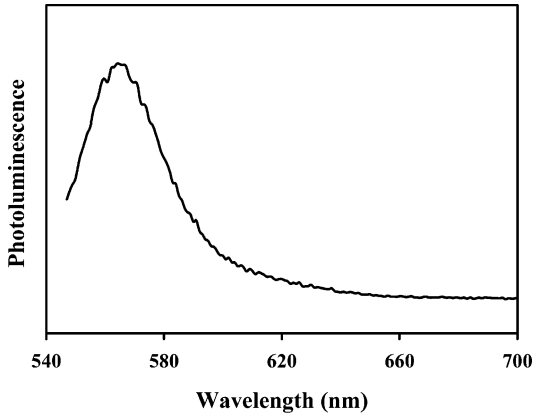

Figure 4. PL spectrum of PAN/rhodamine B/PAN coaxial nanotube (excitation wavelength: 543 nm).

B without the additional PAN layer is diffused into a hydrochloric aqueous solution. On the other hand, the AN monomer is readily polymerized at relatively low temperature (70 °C), and the dye−polymer composite can be fabricated without thermal decomposition of organic dyes.

Figure 4 is the PL spectra of the PAN/rhodamine B/PAN nanotubes excited by 543 nm. The PAN/rhodamine B/PAN nanotube which is precipitated and dried in a vacuum oven is dispersed in spectroscopic grade methanol to obtain the PL spectra. Orange−yellow emission in the wavelength region of 550−600 nm is observed in Figure 4. The PL spectrum of coaxial nanotubes is almost same as that of pure rhodamine B. This result implies that intrinsic properties of organic dyes are maintained in the coaxial nanotube, and the PAN layer with thin wall thickness does not interfere with the emission flux of embedded organic dyes.

Pyrene molecules are adopted to produce coaxial nanotubes with blue emission. It is notable that the pyrene molecules are readily absorbed on an inner site of the AAO membrane coated by PAN with the simple dipping method. Owing to the hydrophobicity of pyrene, these molecules hardly attached to the surface of pristine AAO membranes, which is covered by hydroxyl groups. However, a property of the AAO surface treated with PAN that is displayed is hydrophobicity; therefore, the pyrene molecules can adsorb on the PAN nanotubes. Figure 5a represented 3D CLSM images of the PAN/pyrene/PAN nanotube excited by a 488 nm laser. In Figure 5a, the composite exhibited green emission when the nanotubes were excited by 488 nm and the band path of observation was 505−530 nm. Generally, the color observed in CLSM has some difference with real emission color because the region of observance can be adjusted by controlling the detector band path. Accordingly, despite intrinsic blue emission of the pyrene, green emission is observed. Unfortunately, our CLSM does not support the laser with 334 nm. Instead of CLSM image at 334 nm of excitation wavelength, fluorescence microscope image was obtained with mercury lamps and a band path of 300−400 nm. Although this image is not clear owing to its limitation of resolution, blue emission is obviously observed at the PAN/pyrene/PAN coaxial nanotube (Figure 5b). Figure 5c illustrates the PL spectra of PAN/pyrene/PAN coaxial nanotubes with different pyrene contents (excitation wavelength: 334 nm). The monomer emission peaks of pyrene

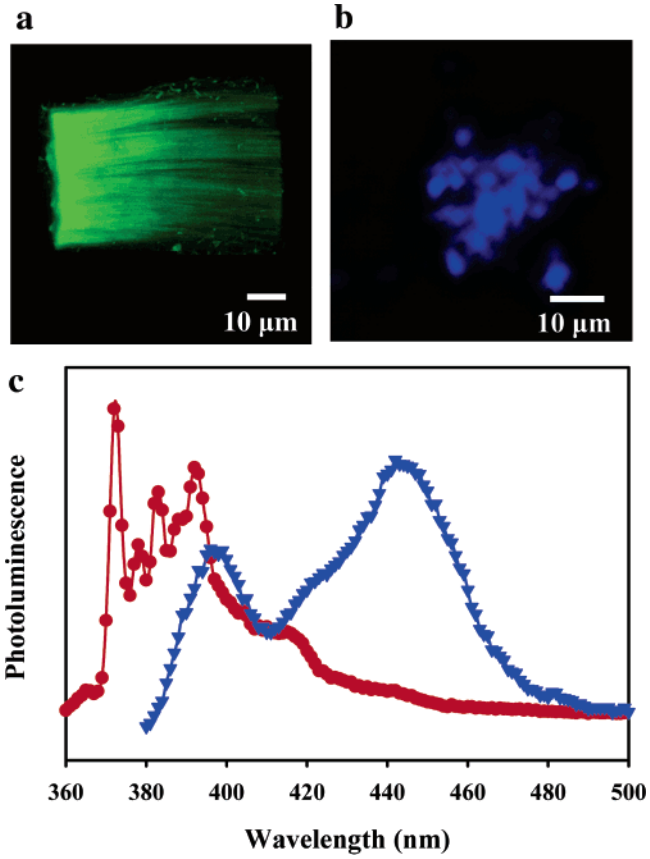

Figure 5. (a) 3D CLSM image of PAN/pyrene/PAN coaxial nanotubes, (b) fluorescence microscope image of PAN/pyrene/PAN coaxial nanotube excited at 365 nm, and (c) PL spectra of PAN/pyrene/PAN coaxial nanotube (excitation wavelength: 334 nm) as a function of pyrene concentration (red circle, 0.1 wt % of pyrene solution; blue inverse triangle, 2 wt %).

at 385 and 374 nm shifted to excimer emission at 470 nm with increasing pyrene concentration (Figure 5c). When the concentration of the pyrene solution was dilute (0.1 wt %), the monomer peak has been mainly observed. The excimer peak appeared according to the increment of the concentration (2 wt %) of dye solution. Remarkably, emission spectra of composite nanotubes depended not on the amount of composite nanotubes in solvent (spectroscopic grade methanol) but on the concentration of dye solution which is used for introducing organic dyes in the synthetic process. It implies that the organic dyes are successfully entrapped in the PAN layers, and protected from environmental factors.

Both rhodamine B and pyrene could also be introduced into the coaxial nanotubes at the same time. Figure 6a,b shows CLSM images of PAN/pyrene−rhodamine B/PAN coaxial nanotubes. In the Figure 6a, pyrene emission is observed when the coaxial nanotubes with dual dyes are excited by 488 nm laser. On the other hand, when the excitation wavelength of the laser changed to 543 nm and the band path of observation moved above 550 nm, red emitting nanotubes have been observed (Figure 6b). The emitting position is almost same as in Figure 6a, and this implies that two organic dyes are dispersed in the PAN coaxial nanotube without phase separation. Comparison of a DIC (differential-interference-contrast) image (not shown) and CLSM images of the composite indicates that PL dyes are restricted

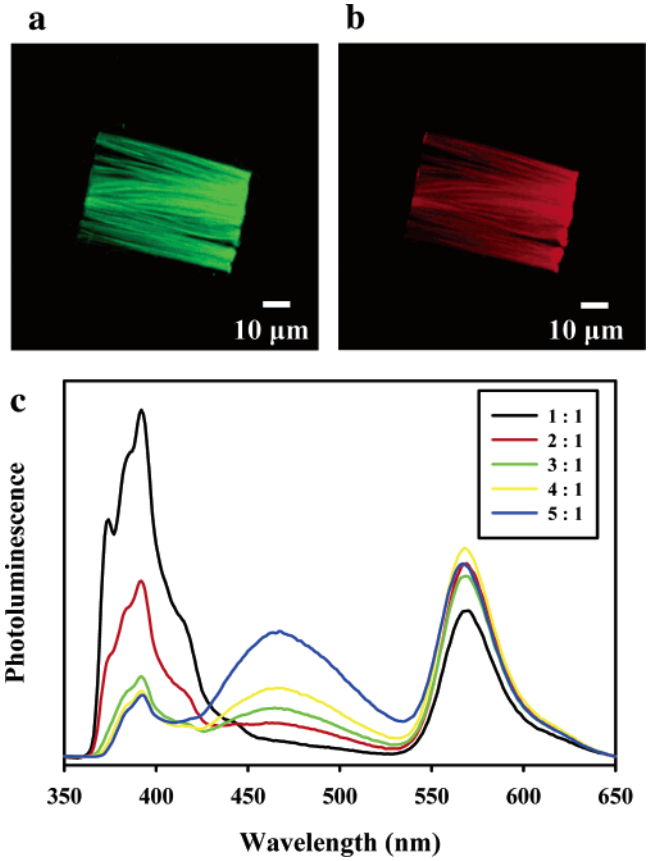

Figure 6. (a) CLSM image of PAN/two dyes/PAN coaxial nanotubes (488 nm laser excitation and band path of observation of 503−530 nm), (b) CLSM images of PAN/two dyes/PAN coaxial nanotubes (543 nm laser and band path of observation of above 550 nm), and (c) PL spectra of PAN/two dyes/PAN (excitation wavelength: 334 nm) as a function of pyrene/rhodamine B weight ratio.

in the nanotubes, and this can be the strong evidence of effective encapsulation of dual organic dyes into the PAN nanotube without any deterioration of organic dyes. Figure 6c describes the PL spectra of PAN/two dyes/PAN coaxial nanotubes with different weight ratios of pyrene and rhodamine B. Typically, rhodamine B has been excited by a wavelength of 543 nm, but a considerable emission can be observed when the excitation wavelength of higher energy (334 nm) is irradiated, even though the efficiency is relatively lower than the case of 543 nm excitation. Accordingly, the PAN/pyrene/rhodamine B/PAN composite which is excited at 334 nm showed diverse emission peaks related with the pyrene and rhodamine B. As shown in Figure 6c, the weight ratio of pyrene and rhodamine B was adjusted by tuning the concentration of dye solution. The amount of pyrene molecules was gradually increased by adding the pyrene to the rhodamine B solution with a certain concentration (1.0×10^{-3} M, typically). When the weight ratio of pyrene and rhodamine B was 1:1, blue and orange−yellow peaks were observed without any interference between both dyes. As the concentration of pyrene increased, excimer emission of pyrene was enhanced. Finally, when the pyrene molecules are rich enough to form the excimer, emission of green (450−500 nm) and orange−yellow is observed. It implies that our facile method proposes universal technology to produce plentiful emission nanotubes with tunable emission color.

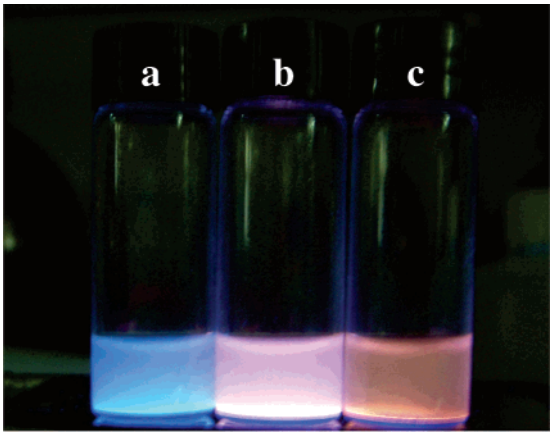

Figure 7. Photograph of PL from dye-embedded polymer nanotubes irradiated by a long wave (365 nm) UV gun: (a) PAN/pyrene/PAN, (b) PAN/two dyes/PAN (1:1 weight ratio of pyrene/rhodamine B), and (c) PAN/rhodamine B/PAN coaxial nanotube.

It is notable that there is also no interference between the two emission peaks. In general, when two organic dyes or fluorescence are encapsulated in a confined dimension, energy transfer occurs from donor to acceptors, resulting in emitting a single color (acceptor's emission). In this system, on the other hand, there is no energy transfer between pyrene and rhodamine B. The following might be responsible for these results: poor spectral overlap between emission of pyrene monomer and absorption of rhodamine B. The large Forster radius, which often indicates large spectral overlap, is an important factor for effective energy transfer. The largest UV−vis absorption of rhodamine B exists in the range of 500−600 nm (maximum peak: 543 nm). Considering that the pyrene emission is mainly at 350−400 nm (400−500 nm of excimer state), the spectral overlap is too weak for energy transfer to occur.

Figure 7 is a photograph which shows the PL of the composite nanotubes incorporating different dyes irradiated by a long wave (365 nm) UV gun. The coaxial nanotube involving pyrene emits blue color, and the rhodamine B-impregnated coaxial nanotube sends out red fluorescence. The nanotubes having two dyes with identical weight ratios of both dyes have a mixture of both emission colors. The emission color of polymer/dye coaxial nanotubes is in good agreement with the PL spectra in Figure 6c. When the chromophores are irradiated by a 365 nm UV lamp, these coaxial nanotubes have the characteristic of multiple emissions with single excitation.

Conclusion

The PAN nanotubes were synthesized using a modified VDP. The VDP with nonreactive vapor can be a facile methodology for fabrication of polymer nanotubes with uniform and tunable wall thickness. These products provide an efficient platform to produce polymer based nanocomposites. In this paper, PL dye embedded PAN nanotubes were fabricated by dipping the AAO template into dye solution and stepwise VDP. When these techniques were used,

multiple emitting nanotubes were produced. Specific functions could be readily introduced into the polymer nanotubes. This methodology might be extended to application for a fluoresceine-labeled DNA carrier and the electro-luminescent nanomaterials of the dye/polymer nanotubes.

Acknowledgment. This work was supported by the Brain-Korea 21 Program (Korea Ministry of Education) and Korea Science and Engineering Foundation through Hyperstructured Organic Materials Research Center.

CM0611542